Hindawi
Advances in High Energy Physics
Volume 2020, Article ID 1852841, 18 pages
https://doi.org/10.1155/2020/1852841

Research Article

Confinement of Fermions in Tachyon Matter

Adamu Issifu[1] **and Francisco A. Brito**[1,2]

[1]*Departamento de Física, Universidade Federal da Paraíba, Caixa Postal 5008, 58051-970 João Pessoa, Paraíba, Brazil*
[2]*Departamento de Física, Universidade Federal de Campina Grande, Caixa Postal 10071, 58429-900 Campina Grande, Paraíba, Brazil*

Correspondence should be addressed to Francisco A. Brito; fabrito@df.ufcg.edu.br

Received 10 December 2019; Accepted 25 March 2020; Published 25 April 2020

Academic Editor: Anna Cimmino

In this paper, we develop a phenomenological model inspired by QCD that mimics the QCD theory. We use the gauge theory in color dielectric medium ($G(\phi)$) coupled with fermion fields to produce scalar and vector confinements in the *chromoelectric flux tube* scenario. The Abelian theory will be used to approximate the non-Abelian QCD theory in a consistent manner. We will calculate vector and scalar glueballs and compare the result to the existing simulation and experimental results and projections. The QCD-like vacuum associated with the model will be calculated and its behavior studied relative to changing quark masses. We will also comment on the relationship between tachyon condensation, dual Higgs mechanism, QCD monopole condensation, and their association with confinement. The behavior of the QCD string tension obtained from the vector potential of the model will be studied to establish vector dominance in confinement theories.

1. Introduction

Scalar and vector confinements [1] in $3+1$ dimensional world have been predicted by hadron spectroscopy [2], by confinement in string picture, and by QCD lattice simulation, but no success has been made in solving it analytically from "first principle" of QCD. It has been shown in quarkonia phenomenology in $3+1$ dimensional world that the best fit for meson spectroscopy is found for a convenient mixture of vector and scalar potentials. The combined vector and scalar potentials have also been studied in many perspectives. The Dirac equation [3, 4] and Schwinger model [5] are among common examples employed to achieve both linear and coulomb-like potentials [6–10]. The attempt to confirm this result predicted by QCD lattice spectroscopy has led to the use of the mass gap equation to generate mass as a dependent parameter even in quark systems with no mass current to create dynamic quarks [11]. Pure scalar and vector potentials have been dealt with in Refs. [12–16] as a point in focus.

In this work, we use the Lagrangian density for confinement of electric field in tachyon matter [17, 18] coupled with fermion fields [18] to produce a Lagrangian density for fermionic tachyons through transformations. In this approach, the dielectric function coupled to the gauge field and the fermion mass produce the needed strong interaction between (anti-)quark pairs and the scalar field ϕ describes the dynamics of the tachyons. We will use a dilaton in gauge theories [19, 20] to determine the coupling constants of the colored particles by transforming the exponential dilaton potential to conform with our chosen tachyon potential considered in this work.

We show that both scalar and vector confinements coincide with the tachyon condensation. This phenomenon is not completely new because tachyon fields play a role similar to Higgs fields where Higgs mechanism proceeds via tachyon condensation [21, 22]. Again, both Higgs and tachyon fields have some properties in common; they are both associated with instability or fast decaying with negative mass squared. The tachyons are expected to condense to a value of order of the string scale. Tachyons with large string couplings are considered charged; in that regard, their condensation leads to dual Higgs mechanism. This naturally translates into confinement in line with the QCD monopole condensation scenario [23]. Moreover, we will compute both vector and scalar glueball masses associated with the model. Glueballs

are simply bound states of pure gluons, mixture of quark and gluon (hybrid), and multiquark bound states. The glueball spectrum has been a subject of interest for some decades now, with the focus on unraveling its states in the context of QCD theory [24].

The success of this type of confinement is based on *Nambu-Goto string* or the *chromoelectric flux tube picture*. The flux tube scenario is generally observed in a static quark frame, such that there is no *chromomagnetic field* to induce the spin-orbit interaction of the quarks. The only interaction that is present, in this case, is the *kinematics Thomas spin-orbit interaction*, which is a relativistic correction. This is true for both vector and scalar confinement potentials, and it is confirmed by lattice simulation results [25]. "*Thomas precession*" is considered scalar; hence, scalar potential is expected but it does not guarantee its connection with the QCD theory. They only relate at long-range spin-orbit interactions of QCD; this is precisely the infrared (IR) regime of the theory. The vector potential is achieved for short-range Thomas spin-orbit interaction, and the scalar potential is consistent with long-range Thomas spin-orbit interaction. Both models do not depend on the quarks' spin-orbit interactions in agreement with the QCD theory [26, 27]. Though, scalar potential models have been phenomenologically accepted and used in many hadron models, it is still struggling to plant its root firmly in fundamental QCD as highlighted in [28, 29]. Eventually, it was established that in a slowly moving quark frame, QCD predicts both spin-dependent [30, 31] and spin-independent [32] relativistic corrections. We will use an Abelian QED throughout the computations, but the color dielectric function $G(r)$ modifies the gauge field and by extension the QCD vacuum of the model [33–35]. We will establish a relationship between the tachyon potential and the color dielectric function in a suitable manner. It is known that the Abelian part of the non-Abelian QCD string tension is 92%; this represents the linear part of the net potential. Thus, we can make an approximation of the non-Abelian field using an Abelian approach [36, 37]—for recent development on this, see [38, 39]. Also, it is established that if Abelian projection is followed as suggested by 't Hooft, non-Abelian QCD is reduced to an Abelian theory with charges and monopoles occurring and when such monopoles condense, confinement results. The idea of monopole condensation is a very useful one. It has been numerically shown that monopole condensation actually occurs in the confinement phase of QCD [40]. Again, the color dielectric function coupled to the gauge field $F^{\mu\nu}F_{\mu\nu}$ contains only low momentum components. Therefore, the use of Abelian approximation is justified in the phenomenological QCD theory. In sum, these properties enable us to apply the phenomenological field theory for QCD in this investigation to establish confinement of quarks and gluons in the infrared regime [7, 40–43].

The color dielectric function G is responsible for the long distance dynamics that bring about confinement in the IR regime of the model. It also facilitates the strong interactions between quarks and gluons. The scalar field $\phi(r)$ is responsible for the dynamics of the self-interacting gluon fields and the color dielectric function. We will use a Lagrangian density that describes the dynamics of the gauge, the scalar field associated with the tachyon, and gluon dynamics and fermion fields coupled with mass at zero temperature [43]. The motivation for using this approach are firstly, we are able to compute both the scalar and vector potentials by considering a heavy antiquark source surrounded by a relatively light and slowly moving quarks. This enables us to compute the effect of short-range spin-dependent "*Thomas precession*" (vector potential) and the effect of long-range spin-independent "*Thomas precession*" (scalar potential). Secondly, we are able to apply the phenomenological effective field theory to identify the color dielectric function with the tachyon potential in a simple form. Also, this approach makes it easy to observe how the QCD vacuum is modified by the dielectric function resulting in gluon condensation. Finally, vector and scalar glueball masses are easily calculated from the tachyon potential and the Lagrangian, respectively.

The paper is organized as follows. In Sec. 2, we review the Maxwell's Lagrangian with the source in color dielectric medium. In Sec. 3, we introduce the Lagrangian density for the model. In Sec. 3.1, we derive the QCD-like vacuum of the model. In Sec. 3.2, we choose a suitable tachyon potential for the study. In Sec. 3.3, we compute the scalar and vector potentials for confinement and vector and scalar glueball masses and explore the physics involved. In Sec. 3.4, we compare our parameters with those from well-known phenomenological models. In Sec. 3.5, we discuss the dual Higgs mechanism associated with the tachyon (and QCD magnetic monopole) condensation and confinement. In Sec. 4, we present the results and analysis. Our final comments are contained in Sec. 5.

2. Maxwell's Equations Modified by Dielectric Function

In this section, we will review the electromagnetic theory in *color dielectric medium*. Beginning with Maxwell's Lagrangian with source

$$\mathscr{L} = -\frac{1}{4}F_{\mu\nu}F^{\mu\nu} - j^{\mu}A_{\mu}, \tag{1}$$

its equations of motion are

$$\partial_{\mu}F^{\mu\nu} = -j^{\nu}. \tag{2}$$

The equations of motion of the electromagnetic field create spherical symmetric solutions similar to the well-known point charge scenario associated with Coulomb's field [44].

Therefore, for electromagnetic field immersed in a dielectric medium $G(\phi)$, where $\phi(r)$ is the scalar field representing the dynamics of the medium, we can construct a Lagrangian density

$$\mathscr{L} = -\frac{1}{4}G(\phi)F_{\mu\nu}F^{\mu\nu} - j^{\mu}A_{\mu}, \tag{3}$$

with its equations of motion given as

$$\partial_{\mu}[G(\phi)F^{\mu\nu}] = -j^{\nu}. \tag{4}$$

We choose the indices to run as $\mu = 1, 2, 3$ and $\nu = 0$. These choices are done carefully to obtain *chromoelectric flux* confinement and to eliminate *chromomagnetic fields* in the rest frame of the particles. As a result, the equation of motion in Equation (4) can be reduced to

$$\nabla\bullet[G(\phi)\mathbf{E}] = j^0 = \rho. \tag{5}$$

By this equation, we have eliminated the effect of magnetic field contributions leaving only the electric field contributions that will run through this paper. From Equation (5), $\mathbf{E}$ is the electric field coupled to the dielectric function $G(\phi)$. Rewriting this equation in spherical coordinates, following the assumption that $E(r)$ and $\phi(r)$ are only functions of r, we get

$$\nabla\bullet[G(\phi)\mathbf{E}] = \frac{1}{r^2}\frac{\partial}{\partial r}\left(r^2 \mathrm{G}(\phi)E_r\right) = \rho. \tag{6}$$

Integrating this differential equation yields

$$\left[r^2 G(\phi)\mathbf{E}\right] = \frac{\rho}{\varepsilon_0}\int_0^R r^2 dr,\ E_r = \frac{q}{4\pi\varepsilon_0 r^2 G(\phi)}, \tag{7}$$

where $q = (4/3)\pi R^3\rho$ and $E = |\mathbf{E}| = E_r$. We observe that the dielectric function modifies the magnitude of the electric field function.

3. Lagrangian Density of the Model

In this paper, we will focus on a model described by a Lagrangian density given by

$$\begin{aligned}\mathscr{L} = &-\frac{1}{4}G(\phi)F_{\mu\nu}F^{\mu\nu} + \frac{1}{2}\partial_\mu\phi\partial^\mu\phi - V(\phi)\\ &-\bar{\psi}\left(i\gamma^\mu\partial_\mu + q\gamma^\mu A_\mu - m_{q\bar{q}}G(\phi)\right)\psi,\end{aligned} \tag{8}$$

where $m_{q\bar{q}}$ is the "bare" quark mass or *current quark mass* when the particles under consideration are light and sometimes referred to as the *running quark mass* if the particles involved are heavy. It should be seen to be the same as the mass term that appear in the QCD Lagrangian [45], while $M(\phi) = m_{q\bar{q}}G(\phi)$ is the constituent quark mass function which will later be identified with the scalar potential $S(r)$ in subsequent sections. The "bare" mass ($m_{q\bar{q}}$) leads to *explicit chiral symmetry* breaking while the $M(r)$ permits both *explicit and dynamical chiral symmetry breaking* similar to renormalized mass in QCD Lagrangian [46–48]; we will discuss it in details subsequently.

It should be noted that due to the mass term together with gauge term, $F_{\mu\nu}F^{\mu\nu}$, the Lagrangian is certain to produce both scalar and vector potential contributions to the fermions. The equations of motion of this Lagrangian density are

$$\partial_\mu\partial^\mu\phi + \frac{1}{4}\frac{\partial G(\phi)}{\partial\phi}F^{\mu\nu}F_{\mu\nu} + \frac{\partial V(\phi)}{\partial\phi} - \bar{\psi}m_{q\bar{q}}\psi\frac{\partial G(\phi)}{\partial\phi} = 0, \tag{9}$$

$$-\left(i\gamma^\mu\partial_\mu + q\gamma^\mu A_\mu\right)\psi + m_{q\bar{q}}G(\phi)\psi = 0, \tag{10}$$

$$\partial_\mu[G(\phi)F^{\mu\nu}] = -\bar{\psi}q\gamma^\nu\psi. \tag{11}$$

Again, the indices are $\nu = 0$ and $\mu = j = 1, 2, 3$ as defined in the previous section. These choices are made deliberately to avoid the creation of the *chromomagnetic field*, so we can focus on the *chromoelectric field* which creates the flux tube picture, relevant for our analysis. Therefore, Equation (11) becomes

$$\nabla\bullet[G(\phi)\mathbf{E}] = \bar{\psi}q\gamma^0\psi = j^0 = \rho, \tag{12}$$

where we have substituted $F^{j0} = -E$. Expressing the above equation in spherical coordinates and integrating the results for electric field solution yields the same result as Equation (7).

Expanding Equation (9) in radial coordinates to ease our analysis, we get

$$-\frac{1}{r^2}\frac{d}{dr}\left[r^2\frac{d\phi}{dr}\right] - \frac{1}{2}\frac{\partial G(\phi)}{\partial\phi}E^2 + \frac{\partial V(\phi)}{\partial\phi} - \bar{\psi}m_{q\bar{q}}\psi\frac{\partial G(\phi)}{\partial\phi} = 0. \tag{13}$$

Here, we replace $F^{\mu\nu}F_{\mu\nu} = -2E^2$ and zero otherwise. This follows from the choice of indices defined above. For simplicity, we will also substitute ($\varepsilon_0 = 1$)

$$\lambda = \frac{q}{4\pi}, \tag{14}$$

thus,

$$\frac{d^2\phi}{dr^2} + \frac{2}{r}\frac{d\phi}{dr} = -\frac{1}{2}\frac{\partial G(\phi)}{\partial\phi}\left[\frac{\lambda}{r^2 G(\phi)}\right]^2 + \frac{\partial V(\phi)}{\partial\phi} - \bar{\psi}m_{q\bar{q}}\psi\frac{\partial G(\phi)}{\partial\phi}, \tag{15}$$

which implies

$$\frac{d^2\phi}{dr^2} + \frac{2}{r}\frac{d\phi}{dr} = \frac{\partial}{\partial\phi}\left[V(\phi) + \frac{\lambda^2}{2}\frac{1}{V(\phi)}\frac{1}{r^4} - \bar{\psi}m_{q\bar{q}}\psi V(\phi)\right]. \tag{16}$$

It has already been established that $G(\phi) = V(\phi)$—see [49, 50] and references therein—for slowly varying tachyons. This result will be used throughout this paper. In the above equation, if we consider a relatively large distance of particle separation from the charge q source, we can ignore the term with λ^2; hence, the equation reduces to

$$\nabla^2\phi = \frac{\partial V(\phi)}{\partial\phi}\left[1 - qm_{q\bar{q}}\delta\left(\vec{r}\right)\right]. \tag{17}$$

We have used the general definition $\bar{\psi}\psi \simeq \rho(r) = q\delta(\vec{r})$ in the above equation.

Switching on the perturbation around the vacuum, $\phi_0 = 1/\alpha$, i.e., $\phi(r) \to \phi_0 + \eta(r)$, here, $\eta(r)$ is a small fluctuation about the true vacuum of the potential, then, Equation (17) becomes

$$\begin{aligned}\nabla^2(\phi_0+\eta) &= \frac{\partial V(\phi)}{\partial\phi}\left(1 - qm_{q\bar{q}}\delta\left(\vec{r}\right)\right)\nabla^2\phi_0 + \nabla^2\eta \\ &= \left(\left.\frac{\partial V}{\partial\phi}\right|_{\phi_0} + \left.\frac{\partial^2 V}{\partial\phi^2}\right|_{\phi_0}\eta\right)\left(1 - qm_{q\bar{q}}\delta\left(\vec{r}\right)\right) \Rightarrow \nabla^2\eta \\ &= 4\alpha^2\left(1 - qm_{q\bar{q}}\delta\left(\vec{r}\right)\right)\eta,\end{aligned} \tag{18}$$

where in the last step, we have used Equation (17) and anticipated the property of the scalar potential that we shall define shortly.

3.1. Determining QCD-like Vacuum and Gluon Condensation. This section will be a continuation of the review under "Gluodynamics and QCD-like Vacuum" contained in Ref. [50, 51]. We know that the Lagrangian for gluodynamics is symmetric under conformal transformation, when treated classically, i.e., $|\varepsilon_v| \longrightarrow 0$. Without any quantum corrections, its energy-momentum tensor trace is zero, $\theta^\mu_\mu = 0$. As a result, it produces vanishing gluon condensate $\langle F^{\mu\nu}F_{\mu\nu}\rangle = 0$, in the classical limit and nonvanishing gluon condensate $\langle F^{\mu\nu}F_{\mu\nu}\rangle \neq 0$, with quantum corrections. Thus, quantum effects distorts the scale invariance [52–56] and brings about QCD energy-momentum tensor ($\theta^{\mu\nu}$) trace anomaly

$$\theta^\mu_\mu = \frac{\beta(g)}{2g}F^{a\mu\nu}F^a_{\mu\nu}, \tag{19}$$

a phenomenon well known in the QCD theory. Here, $\beta(g)$ is the QCD beta-function of the strong coupling g, with a leading term

$$\beta(g) = -\frac{11g^3}{(4\pi)^2}. \tag{20}$$

This model produces vacuum expectation value

$$\left\langle\theta^\mu_\mu\right\rangle = -4|\varepsilon_v|. \tag{21}$$

We will now compute the trace of the energy-momentum tensor from the Lagrangian Equation (8) and compare the result with the result obtained above. This comparison is possible because the third and the fourth terms in Equation (8) clearly break the scale invariant making it possible for comparison with Equation (21). We calculate the energy-momentum tensor trace (θ^μ_μ) by substituting Equation (9) into the expression

$$\theta^\mu_\mu = 4V(\phi) + \phi\Box\phi, \tag{22}$$

and this yields

$$\begin{aligned}\theta^\mu_\mu &= 4V(\phi) - \phi\frac{\partial V}{\partial\phi} - \frac{\phi}{4}\frac{\partial G}{\partial\phi}F^{\mu\nu}F_{\mu\nu} + q\delta\left(\vec{r}\right)m_{q\bar{q}}\phi\frac{\partial G}{\partial\phi} \\ &= 4\tilde{V}' + \tilde{G}'F^{\mu\nu}F_{\mu\nu} - 4q\delta\left(\vec{r}\right)m_{q\bar{q}}\tilde{G}' = 4\tilde{V}_{eff}{}' + \tilde{G}'F_{\mu\nu}F^{\mu\nu}.\end{aligned} \tag{23}$$

Here, we have redefined

$$\tilde{V}' = V - \frac{\phi}{4}\frac{\partial V}{\partial\phi}, \tilde{G}' = -\frac{\phi}{4}\frac{\partial G}{\partial\phi}, \tilde{V}'_{eff} = \tilde{V}' - q\delta\left(\vec{r}\right)m_{q\bar{q}}\tilde{G}'. \tag{24}$$

Comparing Equation (23) to Equation (21), we get

$$\left\langle\tilde{G}'(\phi)F^{\mu\nu}F_{\mu\nu}\right\rangle = -4\left\langle|\varepsilon_v| + \tilde{V}'_{eff}(\phi)\right\rangle. \tag{25}$$

We rescale $\tilde{V}'_{\text{eff}}(\phi)$ to include the vacuum energy density $-|\varepsilon_v|$, i.e.,

$$\tilde{V}'_{\text{eff}} \longrightarrow -|\varepsilon_v|\tilde{V}'_{\text{eff}}, \tag{26}$$

consequently,

$$\left\langle\tilde{G}'(\phi)F^{\mu\nu}F_{\mu\nu}\right\rangle = 4|\varepsilon_v|\left\langle\tilde{V}'_{\text{eff}} - 1\right\rangle. \tag{27}$$

This equation follows the classical limit, where the gluon condensate vanishes when $|\varepsilon_v| \longrightarrow 0$ [57]. Again, we will demonstrate in the subsequent sections that the gluon condensate increases with mass and remains nonvanishing at $m_{q\bar{q}} = 0$, i.e., when the quark mass is "removed" after confinement. This is a consequence of *chromoelectric flux tube* confinement.

3.2. Choosing the Appropriate Tachyon Potential. We select a suitable tachyon potential

$$V(\phi) = \frac{1}{2}\left[(\alpha\phi)^2 - 1\right]^2, \tag{28}$$

which produces tachyon condensation at low energies. This potential follows the restriction

$$V(\phi = \phi_0) = 0, \left.\frac{\partial V}{\partial\phi}\right|_{\phi=\phi_0} = 0, \left.\frac{\partial V}{\partial\phi}\right|_{\phi=0} = 0. \tag{29}$$

These restrictions are necessary to stabilize an asymptotically free system as well as its vacuum [58]. To proceed with the computations, we will require a suitable definition of the three dimensional Dirac delta functions ($\delta(\vec{r})$) that appears in Equation (18). Consequently, we define $\delta(\vec{r})$ in the limit of step function as [59].

$$\delta\left(\vec{r}\right) = \begin{cases} \frac{1}{4\pi}\lim_{R\to 0}\left(\frac{3}{R^3}\right), & \text{if } r \le R, \\ 0, & r > R, \end{cases} \tag{30}$$

where R is the radius of the hadron and r is the interparticle separation distance. Solving Equation (18) in the region $r \le R$, i.e., we are considering the presence of the particles inside the hadron, we get

$$\eta''(r) + \frac{2}{r}\eta'(r) + 2K\eta(r) = 0, \tag{31}$$

where $K = 2((3qm_{q\bar{q}}/4\pi R^3) - 1)\alpha^2$. This equation has solutions given as

$$\eta(r) = \frac{\cosh\left(\sqrt{2|K|}r\right)}{r\alpha\sqrt{|K|}} \text{ and } \eta(r) = \frac{\sin\left(\sqrt{2K}r\right)}{r\alpha\sqrt{K}}, \text{for} \quad r \le R, \tag{32}$$

where $|K| = -K = 2(1 - (3qm_{q\bar{q}}/4\pi R^3))\alpha^2$. Thus, Equation (31) has two different solutions each corresponding to different physical regimes. The hyperbolic cosine represents a solution in the low energy regime (IR regime) while the sine function presents solution in the high energy regime where the particles are asymptotically free (UV regime) and some contribution from the IR regime where the particles is in a confined state. We will consider these solutions separately as we proceed.

Outside the hadron, $r > R$, $\delta(\vec{r}) = 0$, we have

$$\eta''(r) + \frac{2}{r}\eta'(r) + 2K_0\eta(r) = 0, \tag{33}$$

where $K_0 = -2\alpha^2$, which has a solution

$$\eta(r) = \frac{\cosh\left(\sqrt{2|K_0|}r\right)}{\alpha r\sqrt{|K_0|}} \text{ and } \eta(r) = \frac{\sin\left(\sqrt{2K_0}r\right)}{\alpha r\sqrt{K_0}}, \text{ for } r > R. \tag{34}$$

A quark which is kicked out of the pointlike region this way, at relatively high energy, behaves like a massless particle but remains confined to the hadron as would be shown later. For now, we will focus our attention on the solution obtained in the region $r \le R$ (inside the hadron) represented by Equation (32). The color dielectric function for this solution takes the form

$$G(\phi_0 + \eta) = V(\phi_0 + \eta) = V(\phi)\Big|_{\phi_0} + V'(\phi)\Big|_{\phi_0}\eta + \frac{1}{2}V''(\phi)\Big|_{\phi_0}\eta^2 + O(\eta^3) \longrightarrow G(\eta) = V(\eta) = \frac{1}{2}V''(\phi)\Big|_{\phi_0}\eta^2. \tag{35}$$

Tachyon fields are generally unstable with negative mass squared; therefore, it is a common phenomenon to find their vacuum states being unstable. In this case, we choose a potential whose true vacuum is at $V(\phi)|_{\phi_0} = 0$. Switching on perturbation expansion about ϕ_0 will results in a generation of square mass proportional to $V''(\phi)|_{\phi_0}$. This stabilizes the tachyon fields and reduces their velocities significantly, making them viable for analysis in the infrared (IR) regime of the model. Simply put, tachyon fields are naturally associated with instability in the quantum field theory; hence, we perturb the fields about its true vacuum where the potential has its minima. As a result, our perturbation should be understood as a mechanism to stabilize the tachyon fields [60]. Following the above equation, the color dielectric function in the IR regime becomes

$$G(\eta) = 2\alpha^2\eta^2 = \frac{2}{|K|r^2}\cosh^2\left(\sqrt{2\,|\,K\,|}\,r\right). \tag{36}$$

Substituting the above result for $G(\eta)$ into the electric field equation in Equation (7), we get

$$E = \frac{\lambda}{r^2 G} = \frac{\lambda}{r^2\left[(2/r^2\,|\,K\,|)\cosh^2\left(\sqrt{2\,|\,K\,|}\,r\right)\right]}. \tag{37}$$

The same tachyon potential and the procedure adopted here were used in [45] to confine light quarks at a finite temperature. Consequently, the tachyons are expected to generate mass at $V''(\phi)|_{\phi_0}$ leading to a particle-like state resulting in tachyon condensation [61, 62]. It follows that the vacuum stability is independent of the constituent quark mass appearing in the Lagrangian density. These properties observed from this type of potential makes it more efficient for computing confinement potentials and glueball masses for heavy or light (anti-)quark systems. From the aforementioned analysis, we can associate $f_\alpha = 1/\alpha$ to the *decay constant* of the tachyons; the higher its value, the faster the tachyons decay and by extension, the more unstable the QCD-like vacuum created in this process and the vice versa.

3.3. Potentials, Glueball Masses, and Constituent Quark Masses

3.3.1. The Potential of the Particles inside the Hadron. Using the well-known relation for calculating electromagnetic potentials

$$V_c(r) = \mp\int \mathrm{E}\mathrm{d}r, \tag{38}$$

to determine the confinement potential $V_c(r, m_{q\bar{q}})$. Now, we apply the hyperbolic cosine function at the left side of

Equation (32) representing the solution in the IR regime to get

$$V_c(r, m_{q\bar{q}}) = \mp \frac{\lambda\sqrt{|K|}\,\tanh\left[\sqrt{2\,|K|}\,r\right]}{2\sqrt{2}} + c = \mp \frac{\lambda\sqrt{\left(1-\beta q m_{q\bar{q}}\right)}\alpha\,\tanh\left[\sqrt{4\left(1-\beta q m_{q\bar{q}}\right)}\alpha r\right]}{2} + c. \tag{39}$$

Here, β is a constant representing the depth of the delta function well, i.e., $\beta = \delta(R \longrightarrow 0) = 3/(4\pi R^3)$. The above equation gives the net potential observed by massive (anti-)particle pairs ((anti-)quark pairs). In effect, particles of the same kind (two particles or two antiparticles) repel each other while particles of different kinds (particle and antiparticle) attract; for example, color (blue) attracts an anticolor (antiblue) of the same kind or colors of different kinds (blue and green) attract each other and vice versa [12, 63].

We choose the negative part of the potential which corresponds to the potential of an antiparticle. It is appropriate to choose $q = -1$ which also corresponds to an anticharge. We will later find that $q = -1$ is associated with an anticharge which is identifiable with an anticolor charge carried by the gluons. Considering that we are dealing with the potential of an antiparticle, this choice is justifiable. Also, we will choose $R = (3/4\pi)^{1/3}$, i.e., $\beta = 1$ and $c = 0$ (c is the integration constant). Consequently, the net static potential (a combined scalar and vector potentials) seen by an antiparticle confinement in the region $r \le R$, in the rest frame of a heavy source, is given by

$$V_c(r, m) = -\frac{\lambda\sqrt{\left(1+m_{q\bar{q}}\right)}\alpha\,\tanh\left[\sqrt{4\left(1+m_{q\bar{q}}\right)}\alpha r\right]}{2}, \tag{40}$$

and its string tension is given as (the parameters combined as follows are in general related according to the form $(m_{q\bar{q}} + 1/(2\pi\alpha')^{1/2})\tilde{\alpha}^2$, where $\tilde{\alpha}^2 = \alpha^2/(2\pi\alpha')^{1/2}$. This is because the precise relationship between the tachyon potential and color dielectric function is $G(\phi) = (2\pi\alpha')^2 V(\phi)$, where α' is the Regge slope which has dimension of length squared. However, we have assumed $2\pi\alpha' = 1$ along the paper.)

$$\sigma_c\left(m_{q\bar{q}}\right) = -\lambda\left(m_{q\bar{q}} + 1\right)\alpha^2 = \left(m_{q\bar{q}} + 1\right)\alpha^2. \tag{41}$$

The scalar potential contribution here is due to the heavy point-like source situated at the center of the hadron. In this regime or at relatively large interparticle separations r, particles are always confined with hadron degrees of freedom. This result does not present UV effects, i.e., the Coulombic potential effect at $r \longrightarrow 0$. If we choose $\sigma_c \sim 1$ GeV/fm and $\alpha = 0.99$ such that $f_\alpha \simeq 1$, we obtain $m_{q\bar{q}} = 10.10$ MeV, which lies within the range of u and d quark masses. It is important to add that this potential is good for investigating light quarks such as u, d and s quarks, since the potential already lies in the stable regime of the theory where all the quarks are confined into hadrons. Heavy quarks such as c quarks start experiencing the degeneracy (pair production) as shown in Figure 1 with dashed lines. Therefore, this model is recommended for confining light quarks such as u, d, or s only.

This result accounts for both spin-dependent and spin-independent relativistic corrections as QCD predicts for slowly moving quark systems. Because there are spinless quarks (comparatively light) in a slow motion around the heavy point-like antiquark source at the origin. The comotion of the light quarks relative to the central massive static antiquark source creates spin-dependent corrections at short ranges (vector-type interaction) and spin-independent correction at long distances (scalar-type interaction) [64] giving rise to the net potential. To this end, when the surrounding comoving quarks are far away from the heavy source, the string tension that binds them to the massive antiquark source will break leading to pair production (a (anti-)quark pair creation), a phenomenon well known in the QCD theory. However, in the presence of a heavy antiquark source, the new quark created in the process remains attractive towards the original source whereas the new antiquark created in the process remains attractive towards the "break-away" quark. In this regard, the (anti-)quark pairs will always remain confined once there exist, at least, a heavy source. The process remains the same if we consider a heavy quark source as well. This characteristic is depicted by the linear nature of the string tension changing with $m_{q\bar{q}}$ and constant when $m_{q\bar{q}} = 0$.

We will now analyse the behaviour of the particles in the UV regime where the particles are relatively close, i.e., small interparticle separation r, with quark and gluon degrees of freedom. We will use the solution of the sine function at the right side of Equation (32) for this analysis,

$$\eta(r) = \frac{\sin\left(\sqrt{2K}r\right)}{\alpha r\sqrt{K}}. \tag{42}$$

Substituting this result into the color dielectric function, Equation (36) results in

$$G_s(r) = \frac{2}{Kr^2}\,\sin^2\left(\sqrt{2K}r\right). \tag{43}$$

Substituting the above equation into Equation (38),

$$V_s = \int \frac{\lambda}{2r^2\left(\sin\left(\sqrt{2K}r\right)/r\sqrt{K}\right)^2}\,dr, \tag{44}$$

we get

$$V_s(m_{q\bar{q}}, r) = -\frac{\lambda\sqrt{K}\,\cot\left[\sqrt{2K}r\right]}{2\sqrt{2}} + \tilde{c} \simeq -\frac{1}{4r} + \frac{K}{6}r + \tilde{c} \simeq -\frac{1}{4r} + \frac{\left(m_{q\bar{q}} - 1\right)\alpha^2}{3}r + \mathcal{O}\left(r^3\right) + \tilde{c}, \tag{45}$$

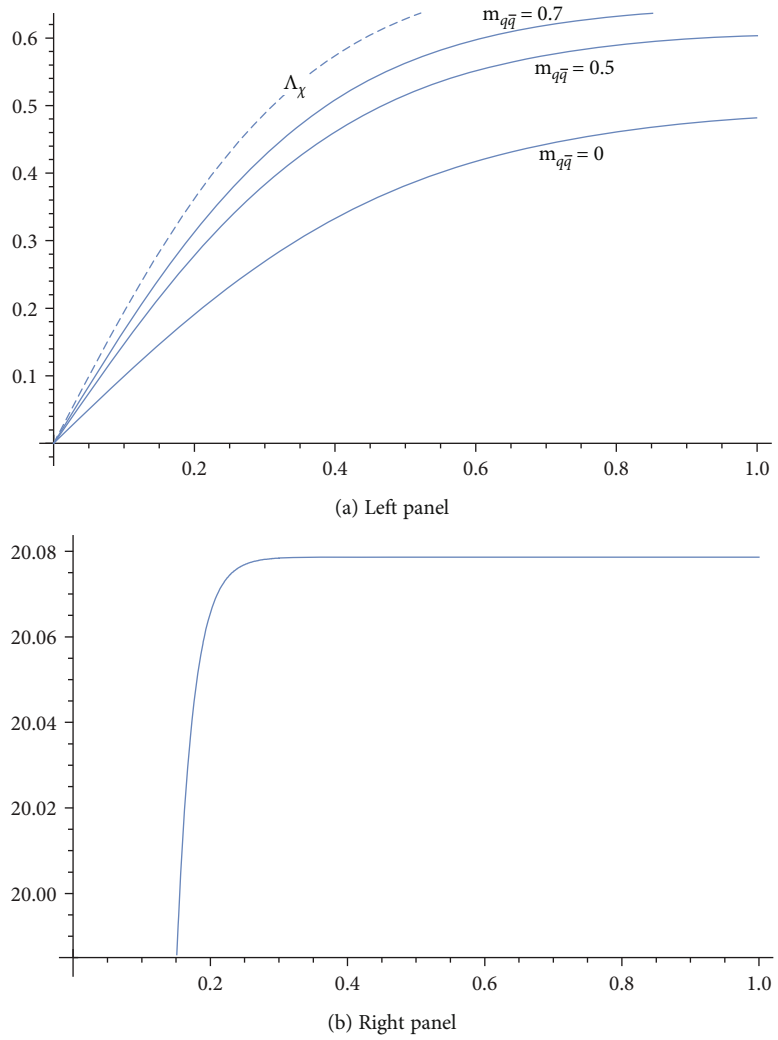

FIGURE 1: A graph of net potential, $V_c(r, m_{q\bar{q}})$, against $(r, m_{q\bar{q}})$ for specific values of $m_{q\bar{q}}$ (a) and an infinite $m_{q\bar{q}}$ (b).

with string tension

$$\sigma_s = \frac{(m_{q\bar{q}} - 1)\alpha^2}{3}, \tag{46}$$

where we have chosen the positive part of the potential corresponding to $\lambda = q = 1$ and $\tilde{c} = 0$. It is known in perturbation QCD that the dominant interaction at small distances, $r \longrightarrow 0$, is Coulombic one-gluon exchange (OGE).

We can estimate the *running quark mass*, $(m_{q\bar{q}})$, using this result, if we consider a typical hadron of mass 1 GeV with radius 1 fm as determined in electron scattering with an estimated string tension σ_s~1 GeV/fm and a decay of $f_\alpha = 1$. We can estimate the *running quark mass* as $m_{q\bar{q}} = 4\,\text{GeV}$, a typical mass for heavy quarks. The mass is slightly less than the mass of a, b quarks, $m_b = 4.18 \pm 0.03\,\text{GeV}$ on mass-independent subtraction scheme ($\bar{\text{MS}}$) at a scale of $\mu = 2$ GeV as reported in the Review of Particle Physics of the Particle Data Group [45]. In addition, light quark masses (such as u, d, and s quark masses) are difficult to determine due to their small masses relative to the hadron scale, so it is sometimes difficult to classify and significantly identify their influence within hadrons. Thus, this model is viable for investigating confinement of quarks with masses $m_{q\bar{q}} \geq 4\,\text{GeV}$; below this threshold, the quarks are expected to be asyptotically free in the UV regime. It is therefore convenient to study the behaviour of light quarks using the IR potential developed in Equation (40), instead of the Cornell-like potential in Equation (45) known for confining heavy quarks [54].

3.3.2. String Tension. Generally, the Cornell potential for confining heavy quarks is given by

$$V(r) = -\frac{e}{r} + \sigma r + V_0, \tag{47}$$

where e and σ are the Cornell fit parameters, but σ is related to the lattice spacing a as $\sigma \sim 1/a^2$ and V_0 is the self energy of the static source. The separation distance, r, between the particles determines the magnitude of a, i.e., large distances imply wide a and vice versa [65]. Determination of e is strictly phenomenological; its larger value corresponds to a smaller mass and vice versa. In relation to our model, we

normalized it at $V_0 = \tilde{c} = 0$, this is to remove the divergence known to be caused by self-energy contribution in the continuum limit and $e = 0.25$ [66]. Unlike the quenched approximation where the particle and antiparticle numbers are independently conserved, in this model, the conserved quantity is the baryon number due to the presence of the *current quark mass* and a *constituent quark mass function*. As would be shown explicitly later, light quark-antiquark pairs are created in the vacuum resulting from the transition in the string tension connecting the two static sources leading to hadronization. When the energy carried by the string tension connecting the two static sources exceeds its critical value at some separation distance $r = r_*$ or some critical mass $m_{q\bar{q}} = m_c$, the string will "break" and decay into light static mesons. Thus, the Coulomb effect e is rather pronounced for higher masses and weaker if the mass involved is slightly weaker than the infrared mass—see the results published in Ref. [67]. Thus, in the limit $r \longrightarrow r_*$, the potentials stop rising with distance r and the static source quark becomes screened by the light quarks formed in the vacuum. Similar behaviour is observed when we keep the distance fixed and increase the mass, i.e., $m_{q\bar{q}} \longrightarrow m_c$. At the ground state, $\sigma_c > \sigma_s$. To obtain confinement, the σ_c can contain a current mass within the range $0 \le m_{q\bar{q}} \le 10.10$ MeV whereas σ_s can contain a current mass within the range $4 \le m_{q\bar{q}} \le m_c$ GeV due to the UV contributions. The running masses for the IR and the UV regimes can be compared with the results of the running masses calculated using various QCD sum rules within the size of a hadron. The masses are given as $\bar{m}_u(1\,\text{GeV}) = 5.2 \pm 0.5$ MeV, $\bar{m}_d(1\,\text{GeV}) = 9.2 \pm 0.5$ MeV, $\bar{m}_s(1\,\text{GeV}) = 159.5 \pm 8.8$ MeV, and $\bar{m}_b(1\,\text{GeV}) = 5.8 \pm 0.06$ GeV [68, 69].

3.3.3. Vector Potential. Using the solution at the left side of Equation (34), i.e., outside the regime of the pointlike source, we will have two separate potential contributions: *vector potential* due to the gluonic sector and the massless quark and a scalar potential energy contribution from the system of the pointlike particles (hadron). Here, the hadron serves as a massive point-like source that confines the massless quark. We will compute the *vector potential* in this section while we reserve the calculations of the *scalar potential energy* and the *net potential energy* for the next section. Using Equations (37) and (38), the vector potential becomes

$$V_v(r) = \mp \frac{\lambda\sqrt{|K_0|}\,\tanh\left[\sqrt{2|K_0|}r\right]}{2\sqrt{2}} + c = \mp \frac{\lambda\alpha\,\tanh\,(2r\alpha)}{2} + c, \tag{48}$$

with string tension

$$\sigma_v = \mp\lambda\alpha^2 = \mp\frac{\lambda}{f_\alpha^2}. \tag{49}$$

This corresponds to the short-range Thomas spin-orbit interactions as highlighted in the introduction. Again, faster tachyon decay means weak string tension while slow decay means strong string tension and stronger confinement. Similar results is obtained if we set $m_{q\bar{q}} = 0$ in Equation (39).

3.3.4. Scalar Potential. To determine the resulting scalar potential due to the hadron, we compare our results from Equation (10) with the generalized Dirac equation where the scalar and the vector potentials coexist as

$$\left[c\widehat{\alpha}\widehat{p} + \widehat{\beta}m_0c^2 + V(r)\right]\psi = 0. \tag{50}$$

Here, we have used $P^\mu = ((E/c), \vec{P})$, $A^\mu = (\Phi(r), \vec{A})$; assuming that the quarks are scalar (spinless) and static, we have $E = \vec{A} = \Phi(r) = 0$. In spherical wall potential, we can impose the restriction

$$V(r) = \begin{cases} S(r), & \text{for } r \le R, \\ 0, & \text{for } r > R, \end{cases} \tag{51}$$

where r is the interquark separations and R is the radius of the hadron. Here, $V(r) = S(r)$ represents the scalar potential in the Dirac equation. Thus, Equation (50) can be rewritten as

$$\left(c\widehat{\alpha}\widehat{p} + \widehat{\beta}m_0c^2\right)\psi + S(r)\psi = 0, \tag{52}$$

where $\widehat{\alpha}$ and $\widehat{\beta}$ are Dirac matrices. Also, $\widehat{p} \longrightarrow -i\nabla$ ($\hbar = 1$) is the momentum operator, m_0 is the rest mass of the fermions, and c is the speed of light in vacuum. The vector potential is normally introduced by minimal substitution of the momentum $P_\mu \longrightarrow P_\mu - gA_\mu$ while the scalar potential is introduced by the mass term $m \longrightarrow m_0 + S$, where g is a real coupling constant. It should be noted that the vector and scalar potentials are coupled differently in the Dirac equation (57). Comparing Equation (10) and Equation (52), we can identify the first and second terms of both equations as the interaction terms and the third terms as the scalar potentials [70, 71]. We leave out the vector potential because it has already been calculated in Sec.3.3.3, so it is of no further interest. The resulting scalar potential seen by the fermions is

$$\begin{aligned} S\left(r, m_{q\bar{q}}\right) = m_{q\bar{q}}G(r) &= \frac{1}{2}m_{q\bar{q}}V''(\phi)\Big|_{\phi_0}\eta^2(r) \\ &= 2m_{q\bar{q}}\alpha^2\eta^2 = m_{q\bar{q}}\left[\frac{2}{r^2\,|\,K\,|}\,\cosh^2\left(\sqrt{2\,|\,K\,|}\,r\right)\right]. \end{aligned} \tag{53}$$

This result represents Thomas spin-orbit interactions at long ranges, whereas the short-range Thomas spin-orbit interactions are partially dominated giving way to scalar interactions only. As a result, the interactions are thought of as being concentrated on the various quark coordinates. Interestingly, the *scalar potential energy* is simply a product of $m_{q\bar{q}}$ and the color dielectric function. This gives an

indication that confinement in this scenario has a direct relation with tachyon condensation and $m_{q\bar{q}}$ of the system.

Meanwhile, some authors have predicted vector dominance over scalar for interquark potentials, suggesting that scalar dominance will imply that all quark combinations are confined. Contrary to that, only the energetic combinations are preferred phenomenologically [12]. We will attempt to analyse this assertion by computing and comparing the magnitudes of their coupling constants as they are expected to appear in the Dirac equation and its significance. The net confining potential energy of a quark outside the hadron will be the sum of Equations (48) and (53) yielding

$$\mathrm{V}_{\mathrm{net}}(r,m) = \pm\frac{q^2\alpha\tanh(2\alpha r)}{8\pi} + \frac{m_{q\bar{q}}}{r^2\left(1+m_{q\bar{q}}\right)\alpha^2}\cosh^2\left(\sqrt{4\left(1+m_{q\bar{q}}\right)}\alpha r\right). \tag{54}$$

Here, we have multiplied the vector potential in Equation (48) with an antiparticle charge $-q$ to obtain a vector potential energy that goes into the net potential energy.

To end this section, we will present the color dielectric function and the scalar potential for the sine function used in investigating the particles inside the hadron in the UV regime. Consequently, the color dielectric function will be

$$G_s\left(r,m_{q\bar{q}}\right) = \left[4-\frac{8K}{3}r^2\right] = \left[4-\frac{16\left(m_{q\bar{q}}-1\right)\alpha^2}{3}r^2\right], \tag{55}$$

and the scalar potential of the hadron reads

$$S_s\left(r,m_{q\bar{q}}\right) = m_{q\bar{q}}\left[4-\frac{8K}{3}r^2\right] = m_{q\bar{q}}\left[4-\frac{16\left(m_{q\bar{q}}-1\right)\alpha^2}{3}r^2\right], \tag{56}$$

for $\lambda = q = 1$.

3.3.5. Glueball Masses. This model is certain to produce both vector and scalar glueballs just as vector and scalar potentials calculated above. Scalar glueball mass has been estimated to have a value within the range 1.5 to 1.7 GeV. This value has been affirmed by data and calculations [72]. A specific value was reached in Ref. [73] to be 1.7 GeV for fitness, through unquenched calculation. On the other hand, the existence of vector glueball mass has been predicted with an estimated value of 3.8 GeV by quenched lattice QCD [74]. The vector glueball masses are expected to be observed at the ongoing Beijing Spectrometer Experiment (BESIII) and hopefully future PANDA experiment at the FAIR Lab [70]. Recent findings published by BESIII facility [71] point to vector particles of mass 3.77 to 4.60 GeV with precision.

From the tachyon potential in Equation (28), we can directly calculate the "vector glueball" mass (m_{gb}) as

$$m_{gb}^2 = \left.\frac{\partial^2 V}{\partial\phi^2}\right|_{\phi_0} = 4\alpha^2. \tag{57}$$

The scalar glueball mass is then calculated directly from the Lagrangian in Equation (8) as

$$m_{gb\phi}^2 = -\left\langle\frac{\partial^2\mathscr{L}}{\partial\phi^2}\right\rangle\Big|_{\phi_0} = 4\alpha^2\left(1+m_{q\bar{q}}\right) + \alpha^2\left\langle F^{\mu\nu}F_{\mu\nu}\right\rangle\Big|_{\phi_0} = 4\sigma_c, \tag{58}$$

where we have substituted $\psi\bar{\psi} = q\delta(\vec{r}) \longrightarrow q\beta$, $q=-1$, and $\beta = 1$. Following the analysis in Sec. 3.1, we find that $\left\langle F^{\mu\nu}F_{\mu\nu}\right\rangle\big|_{\phi_0} = 0$. Therefore, the model produces vanishing gluon condensate in its vacuum (ϕ_0). We can now rewrite Equation (58) in terms of the string tension σ_c and the vector glueball mass as

$$m_{gb\phi}^2 = \frac{m_{gb}^2\sigma_c}{\alpha^2} = m_{gb}^2\sigma_c f_\alpha^2. \tag{59}$$

From the aforementioned analyses, we find that the vector and scalar glueballs depend on the tachyon decay constant, $\alpha = 1/f_\alpha$. While the vector glueball depends directly on f_α, the scalar glueball only depends on f_α through the string tension σ_c. Knowing the estimated values of scalar and the vector glueball masses and the value of the string tension σ_c~1 GeV/fm, we can fix the tachyon decay constant within the range, $0 < f_\alpha \leq 1$. If we consider that the tachyons are decaying at half of its maximum value, i.e., $f_\alpha = 0.5$, we will obtain $m_{gb\phi} = 2$ GeV and $m_{gb} = 4$ GeV. This decay regime gives a good agreement with the vector glueball mass within the range of the experimental values. That notwithstanding, vector and scalar glueballs are more likely to be observed for slowly decaying tachyons.

3.3.6. Constituent Quark Masses. We would like to make brief comments on the constituent quark mass function $M(\phi)$ that was mentioned below Equation (8). This function is the same as the scalar potential energy $S(r)$ determined from the Dirac equation and discussed under Sec. 3.3.4. Here, we will seek to determine its value for $r \longrightarrow 0$ and $r \longrightarrow r_*$, i.e., the excited state and the ground state, respectively.

Now, expanding the solution for the hyperbolic cosine in Equation (32) for $\sqrt{2\,|K|}\,r \ll 1$, we get

$$\eta(r) = \frac{\cosh\left(\sqrt{2\,|K|}\,r\right)}{r\alpha\sqrt{|K|}} \simeq \frac{1}{r\alpha\sqrt{|K|}}\left[1+|K|\,r^2\right] + O\left(r^3\right). \tag{60}$$

Using the expression for $G(\eta)$ in Equation (36) and the

above solution, we can write

$$M(r) = \frac{2m_{q\bar{q}}}{r^2 \mid K \mid}\left[1 + 2 \mid K \mid r^2\right] + \mathcal{O}\left(r^3\right) = \frac{2m_{q\bar{q}}}{r^2 \mid K \mid} + 4m_{q\bar{q}} + \mathcal{O}\left(r^3\right). \tag{61}$$

Thus, the constituent quark mass for the ground-state energy will be $M(r \longrightarrow r_*) = 4m_{q\bar{q}}$ [66], where r_* represents the distance within which the quarks are confined and beyond it, we have degeneracy. Therefore, the constituent quark mass (M_{r_*}) for the potential in Equation (40) is 40.4 MeV, and degeneracy should be expected beyond this mass limit.

We can now proceed to equivalently calculate the constituent quark mass (M_0) for the highest excited state $r \longrightarrow 0$ by using the sine function solution in Equation (32), this yields

$$M(r) = 4m_{q\bar{q}}\left[1 - \frac{Kr^2}{3}\right] + \mathcal{O}\left(r^3\right). \tag{62}$$

Therefore, $M(r \to 0) = 4m_{q\bar{q}}$ is the constituent quark mass in this regime; if we choose a running quark mass of $m_{q\bar{q}} = 4\,\text{GeV}$ as calculated above, we get, $M_0 = 16\,\text{GeV}$. So, the constituent mass (M) in this model framework lies between $0 \le M \le 16\,\text{GeV}$, where $0 \le M_{r_*} \le 40.4\,\text{MeV}$ gives the dynamics of the IR regime while the UV regime can be studied within $4 \le M_0 \le 16\,\text{GeV}$.

The quark masses that appear in phenomenological models are generally the *constituent quark mass* [45] which dynamically breaks the chiral symmetry. In nonperturbative theories, the range for *dynamical chiral symmetry* breaking, Λ_χ, is about 1 GeV [75]. It is therefore conventional to say a quark is heavy if $M > \Lambda_\chi$; in this case, we have *explicit chiral symmetry breaking* for *c*, *b*, and *t* quarks while quarks are classified as light if $M < \Lambda_\chi$, leading to *spontaneous chiral symmetry breaking* dominance. Quarks in this category include *u*, *d*, and *s*. In nonrelativistic quark models, one of the useful parameters is the constituent quark mass which is determined to be $M_u = M_d = 350\,\text{MeV}$ for light quarks in *single gluon exchange* (OGE) interaction, while the predicted mass for a *c* quark is also $M_c = 1.6\,\text{GeV}$. Constituent quark mass models are used to study the effect of *dynamical chiral symmetry breaking*, and they are independent of the *current quark mass*. The *constituent quark mass* changes depending on how measurements are made in a particular model framework. The constituent quark masses are greater compared to the *current quark mass* and are usually free parameters to fit in potential models. The masses vary depending on whether you are using a meson fits, baryon fits, hadron fits, or other phenomenological models.

3.4. Identification of Coupling Constants. In this section, we will compare the result from Equation (16) with the well-known phenomenological models [12, 76], using dilaton in the gauge theory to confine quarks and gluons with N_c colors. For emphasis, since our model is phenomenological, it lacks all the degrees of freedom required to fully represent the pure QCD theory, but our results agree with the QCD spectrum for scalar and vector potentials.

The results presented above still keeps the electromagnetic charge q and do not contain the color numbers N_c. This comparison is intended to help fill in these gaps. Furthermore, the scalar and the vector potentials in the Dirac equation are of the same weight but coupled differently. This comparison will enable us to determine their couplings and relate them to their individual strengths in the QCD-like model. The same method was used in [49]—and references herein—to determine couplings as well. The dilaton model is given as

$$\frac{d^2\phi}{dr^2} + \frac{2}{r}\frac{d\phi}{dr} = -\frac{g^2}{64\pi^2 f_\phi}\left(1 - \frac{1}{N_c}\right)\exp\left(-\frac{\phi}{f_\phi}\right)\frac{1}{r^4} - \frac{\xi}{2f_\phi}\exp\left(-\xi\frac{\phi}{2f_\phi}\right)m_{q\bar{q}}g\delta(r). \tag{63}$$

Transforming the exponential potentials of the above equation to conform with the tachyon potential used, i.e, $\exp\left(-((\phi(r))/f_\phi)\right) \longrightarrow 2(\alpha^4\phi^3 - \alpha^2\phi)$ and $\exp\left(-\xi((\phi(r))/2 f_\phi)\right) \longrightarrow 2(((\alpha^4\phi^3\xi^4)/16) - ((\alpha^2\phi\xi^2)/4))$; hence, Equation (63) can be rewritten as

$$\frac{d^2\phi}{dr^2} + \frac{2}{r}\frac{d\phi}{dr} = \frac{g^2}{32\pi^2 f_\phi}\left(1 - \frac{1}{N_c}\right)\frac{\alpha^2\phi}{r^4} + \frac{2\xi^3\alpha^2\phi}{8f_\phi}m_{q\bar{q}}g\delta(r). \tag{64}$$

It should be noted that the purpose of this section is to determine the coupling constants, so the equations have been simplified to achieve that goal.

Comparing Equations (16) and (64), we can find $\xi = 2$, and $\alpha^2 = 1/f_\phi = 1/f_\alpha^2$. Here, ξ represents the coupling strength of the fermions; f_ϕ is the mass decay constant of the dilaton and it is related to the decay constant of the tachyons f_α; g is the gluon charge and it is related to the electromagnetic charge q. We can rewrite Equations (14), (40), and (41) as

$$\lambda = -\frac{g}{2\pi}\left(1 - \frac{1}{N_c}\right)^{1/2}, q = -g\sqrt{\left(1 - \frac{1}{N_c}\right)}, \tag{65}$$

$$V_c\left(r, m_{q\bar{q}}\right) = \frac{g}{4\pi}\sqrt{\left(1 - \frac{1}{N_c}\right)}\frac{\sqrt{\left(1 + m_{q\bar{q}}\right)}\alpha\tanh\left[\sqrt{4\left(1 + m_{q\bar{q}}\right)}\alpha r\right]}{2}, \tag{66}$$

$$\sigma_c\left(m_{q\bar{q}}\right) = \frac{g}{4\pi}\sqrt{\left(1 - \frac{1}{N_c}\right)}\left(m_{q\bar{q}} + 1\right)\alpha, \tag{67}$$

for $g \longrightarrow g/(2\sqrt{2})$, respectively.

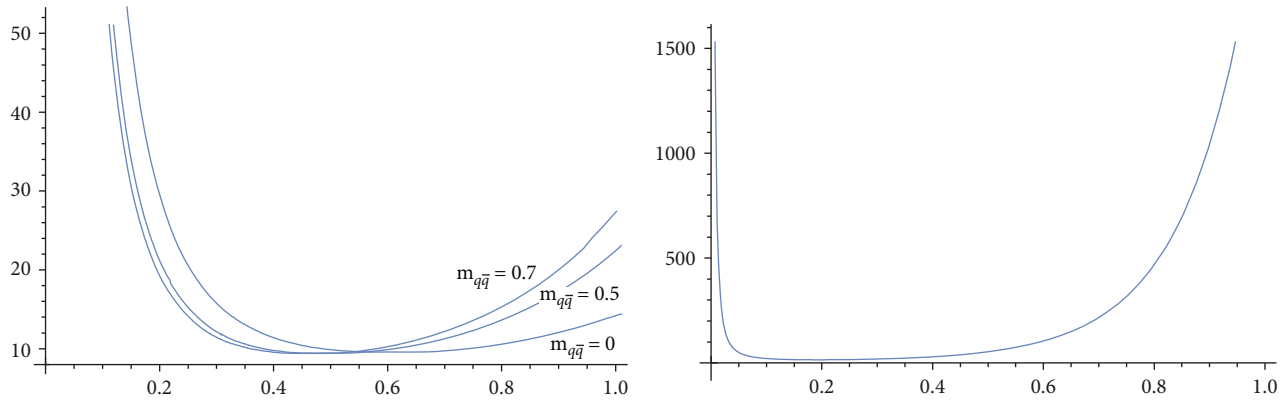

(a) Left panel (b) Right panel

FIGURE 2: A graph for color dielectric function, $G(r, m_{q\bar{q}})$, against $(r, m_{q\bar{q}})$ for specific values of $m_{q\bar{q}}$ (a) and for infinite $m_{q\bar{q}}$ (b).

The *scalar potential energy* observed by the heavy point-like antiquark source is also given as

$$S\left(r, m_{q\bar{q}}\right) = 2m_{q\bar{q}}\alpha^2\eta(r)^2 = m_{q\bar{q}}\left[\frac{1}{r^2\left(1+m_{q\bar{q}}\right)\alpha}\cosh^2\left(2\sqrt{\left(1+m_{q\bar{q}}\right)}\alpha r\right)\right]. \quad (68)$$

We find from the above Equation (36) for the dielectric function G that the larger the quark mass the more stable the QCD-like vacuum and the faster the tachyons condense [77]. Since tachyon condensation implies confinement, then heavier quarks are more likely to be confined than light quarks [78]. This potential follows the same analysis as the dielectric function with the tachyons condensing faster in a multiple of $m_{q\bar{q}}$ showing a rather stronger confinement but vanishes at $m_{q\bar{q}} = 0$. This result represents the energy flow between a quark and an antiquark pairs at long ranges. On the other hand, Equation (66) represents the *net potential* for confinement observed for a heavy antiquark source in the origin surrounded by relatively light spinless quarks in a slow motion.

It is important to state that the net confinement potential seen in Equation (66) corresponds to a mixture of $\xi = 0$ (no mass coupling) and $\xi = 1$ (Kaluza-Klein-type or mass coupling) [79]. The combined $\xi = 1$ and $\xi = 0$ give the net confinement of the quarks at all masses inside the hadron. Also, Equation (68) gives the *scalar potential energy*, i.e., the flow of energy between two or more quarks. The coupling of the scalar potential, $\xi = 2$, exposes its weakness relative to the vector potential in Equation (48) by a ratio of 0 : 2. By simple interpretation, the scalar potential energy must be coupled strongly in order to coexist with the vector potential energy which needs no coupling as seen in our model framework and presented in expression Equation (54). It is noticeable that the scalar potential energy vanishes at $m_{q\bar{q}} = 0$ while the vector potential energy does not as evidenced in Equation (54). Consequently, quarks are always in a confined state [80–83] under the net confining potential Equation (66) and at $m_{q\bar{q}} = 0$, we retrieve the vector potential Equation (48). This indicates that the *chromoelectric flux* generated by the colored particles remains confined even if we "remove" the quarks after confinement under the net confining potential (V_c) [2]. It should be noted also that the net confinement potential of the color particles is the sum of the vector and the scalar potentials as presented in (66) and the net potential energy is also the sum of the vector and scalar potential energies as expressed in Equation (54). After knowing all the coupling constants and the nature of the Dirac delta function, few comments on Sec. 3.1 will be necessary. Noting that the Dirac delta function is well defined inside the hadron $r \le R$, with depth $\beta = 3/(4\pi R^3) = 1$, $G(\phi) = V(\phi)$, and an antigluon color charge $q \longrightarrow g = -1(N_c \gg 1)$, Equation (24) takes the form

$$\tilde{V}'_{eff}(\phi) = \tilde{V}' - q\delta(r)m_{\bar{q}q}\tilde{G}' = V - \frac{\phi}{4}\frac{\partial V}{\partial\phi} + m_{q\bar{q}}\left(-\frac{\phi}{4}\frac{\partial G}{\partial\phi}\right) = V - \frac{\phi}{4}\frac{\partial V}{\partial\phi}\left(m_{q\bar{q}}+1\right). \quad (69)$$

Substituting Equation (35), recalling that $V(\eta(r)) = G(\eta(r)) = 2\alpha^2\eta^2$ for $\phi(r) \longrightarrow \phi_0 + \eta(r)$, into the above expression yields

$$\tilde{V}'_{eff} = 2\alpha^2\eta^2 - (\phi_0+\eta)\alpha^2\eta\left(m_{q\bar{q}}+1\right) = \alpha^2\eta^2\left(1-m_{q\bar{q}}\right) - \phi_0\alpha^2\eta\left(1+m_{q\bar{q}}\right) = \alpha^2\eta^2\left(\left(1-m_{q\bar{q}}\right) - \alpha\eta\left(1+m_{q\bar{q}}\right)\right. \text{for } \alpha = 1/\phi_0. \quad (70)$$

Since tachyon condensation is faster when $\tilde{V}'_{eff} \longrightarrow 0$, see Figure 2, tachyons condense with increasing mass and attain its minimum condensation at $m_{q\bar{q}} = 0$ corresponding to the maximum value of $\tilde{V}'$. As a results, Eq. (27) yields

$$\left\langle(\phi_0+\eta)G'(\eta)F_{\mu\nu}F^{\mu\nu}\right\rangle = 16|\varepsilon_v|\left\langle 1-\alpha^2\eta^2\left(1-m_{q\bar{q}}\right)\right\rangle + 16|\varepsilon_v|\left\langle\alpha\eta\left(1+m_{q\bar{q}}\right)\right\rangle \longrightarrow \left\langle\left(\alpha\eta+\alpha^2\eta^2\right)F_{\mu\nu}F^{\mu\nu}\right\rangle = 4|\varepsilon_v|\left\langle 1-\alpha^2\eta^2\left(1-m_{q\bar{q}}\right)\right\rangle + 4|\varepsilon_v|\left\langle\alpha\eta\left(1+m_{q\bar{q}}\right)\right\rangle. \quad (71)$$

By this result, tachyon condensation increases with the increasing mass $m_{q\bar{q}}$ and attains its minimum when $m_{q\bar{q}} = 0$. There is a QCD monopole condensation associated with both instances (i.e., $m_{q\bar{q}} = 0$ and $m_{q\bar{q}} > 0$), since the gluon condensates do not vanish in any of the two instances. The condensate is higher with increasing mass and relatively low at no mass. Naturally, confinement results in both instances.

3.5. Tachyon Condensation and Dual Abelian Higgs Mechanism. For the sake of simplicity, but without lost of generality, in the previous sections, we have postponed the discussion concerning the dual description of the confinement in terms of the Higgs mechanism. We shall now complete the discussion by extending the the Lagrangian in Equation (8) by imposing gauge invariance on the scalar sector. As such, the degrees of freedom should be carefully changed. Firstly, we have to consider a charged scalar field, i.e., a complex scalar field

$$\phi = \frac{\phi_1 + i\phi_2}{\sqrt{2}}. \tag{72}$$

We will leave out the fermion (spinors) coupling from the original Lagrangian in Equation (8) for this analyses because it has no direct influence on the outcome of the intended result. Consequently,

$$\mathscr{L} = -\frac{1}{4} G(|\phi|) F_{\mu\nu} F^{\mu\nu} + D_\mu \phi D^\mu \phi^* - \frac{1}{4} \tilde{F}_{\mu\nu} \tilde{F}^{\mu\nu} - V(|\phi|), \tag{73}$$

where $F_{\mu\nu} = \partial_\mu A_\nu - \partial_\nu A_\mu$ and $\tilde{F}_{\mu\nu} = \partial_\mu \tilde{A}_\nu - \partial_\nu \tilde{A}_\mu$ are two independent Abelian field strengths and $D_\mu = \partial_\mu - iq\tilde{A}_\mu$ is the Abelian covariant derivative associated with the *dual* gauge field $\tilde{A}_\mu$ which is responsible for the magnetic monopole description in the dual Higgs mechanism. Besides its original $U(1)$ gauge invariance, the Lagrangian becomes invariant under the following $\tilde{U}(1)$ gauge transformation

$$\phi(x) \longrightarrow \phi'(x) = e^{iq\alpha(x)} \phi \tilde{A}(x) \longrightarrow \tilde{A}'(x) = \tilde{A}(x) - \partial_\mu \alpha(x). \tag{74}$$

We can now analyze the dual Higgs mechanism of the model. Going forward, the potential of the model in Equation (28) will also take the form

$$V(|\phi|) = 2\alpha^4 (\phi\phi^*)^2 - 2\alpha^2 \phi\phi^* + \frac{1}{2}. \tag{75}$$

The minima of this potential function is given as

$$\frac{\partial V}{\partial \phi^*} = 0 \longrightarrow 4\alpha^4 (\phi\phi^*)\phi - 2\alpha^2 \phi = 0, \langle |\phi| \rangle_0 = \sqrt{\phi_0 \phi_0^*} = \sqrt{\frac{1}{2\alpha^2}}. \tag{76}$$

The nonzero vacuum expectation value breaks the $\tilde{U}(1)$ gauge symmetry spontaneously.

Let us now proceed as in our previous analyses by expanding about the vacuum of the potential so, for ease of calculations, we choose physical vacuum configuration

$$\phi_{1\min} = \phi_0, \text{ and } \phi_{2\min} = 0. \tag{77}$$

Now, we choose two real scalar fields $\eta(r)$ and $\zeta(r)$ [84, 85] to represent small fluctuations about the vacuum of the potential.

So we can represent the shifted vacuum as

$$\phi = \eta + \langle \phi \rangle_0. \tag{78}$$

As such, we can conveniently parametrize the ϕ field as

$$\phi = e^{i\zeta/\phi_0} \frac{(\phi_0 + \eta)}{\sqrt{2}} \approx \frac{(\phi_0 + \eta(r) + i\zeta(r))}{\sqrt{2}}. \tag{79}$$

The Lagrangian for the small fluctuations about the vacuum up to quadratic order becomes

$$\begin{aligned} \mathscr{L} = {} & \frac{1}{2} \left[\partial_\mu \eta \partial^\mu \eta - 4\alpha^2 \eta^2 \right] \\ & + \frac{1}{2} \left[\partial_\mu \zeta \partial^\mu \zeta - 2q\phi_0 \tilde{A}_\mu \partial^\mu \zeta + q^2 \phi_0^2 \tilde{A}_\mu \tilde{A}^\mu \right] \\ & - \frac{1}{4} G(\eta) F_{\mu\nu} F^{\mu\nu} - \frac{1}{4} \tilde{F}_{\mu\nu} \tilde{F}^{\mu\nu} + \cdots. \end{aligned} \tag{80}$$

Notice that the scalar field η plays the role of the usual massive Abelian Higgs field and the scalar field ζ is related to the massless Goldstone boson. Now choosing the gauge,

$$\tilde{A}_\mu \longrightarrow \tilde{A}' = \tilde{A}_\mu - \frac{1}{q\phi_0} \partial_\mu \zeta, \tag{81}$$

we can write

$$\begin{aligned} & \frac{1}{2} \partial_\mu \zeta \partial^\mu \zeta - q\phi_0 \tilde{A}_\mu \partial^\mu \zeta + \frac{q^2 \phi_0^2}{2} \tilde{A}_\mu \tilde{A}^\mu \\ & \quad = \frac{q^2 \phi_0^2}{2} \left[\tilde{A}_\mu - \frac{1}{q\phi_0} \partial_\mu \zeta \right] \left[\tilde{A}^\mu - \frac{1}{q\phi_0} \partial^\mu \zeta \right] \\ & \quad = \frac{q^2 \phi_0^2}{2} \tilde{A}'_\mu \tilde{A}'^\mu. \end{aligned} \tag{82}$$

Thus, the Lagrangian takes the form

$$\begin{aligned} \mathscr{L} = {} & -\frac{1}{4} G(\eta) F_{\mu\nu} F^{\mu\nu} + \frac{1}{2} \partial_\mu \eta \partial^\mu \eta - V(\eta) \\ & - \frac{1}{4} \tilde{F}'_{\mu\nu} \tilde{F}'^{\mu\nu} + \frac{q^2 \phi_0^2}{2} \tilde{A}'_\mu \tilde{A}'^\mu + \cdots. \end{aligned} \tag{83}$$

This is precisely the Lagrangian (8) evaluated around the vacuum plus the Lagrangian of the dual gauge field. Notice that $G(\eta) = V(\eta) = 2\alpha^2 \eta^2$ is consistent with (35). Furthermore, as we have well discussed in the previous sections, in the limit $\eta \longrightarrow 0$, we have tachyon condensation and confinement. Then at such a limit, we are left with the Lagrangian

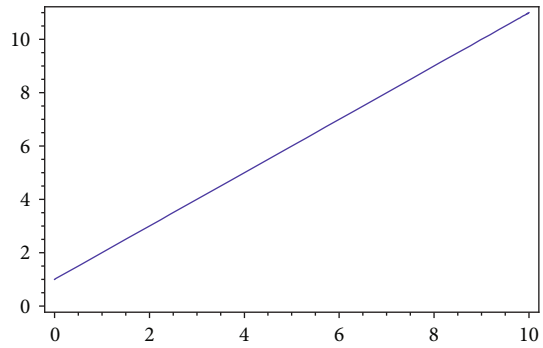

FIGURE 3: A graph of string tension $\sigma_c(m_{q\bar{q}})$ against mass, $m_{q\bar{q}}$, for a heavy antiquark source.

$$\tilde{\mathscr{L}} = -\frac{1}{4}\tilde{F}'_{\mu\nu}\tilde{F}'^{\mu\nu} + \frac{q^2\phi_0^2}{2}\tilde{A}'_{\mu}\tilde{A}'^{\mu}, \tag{84}$$

which describes the dynamics of a massive dual gauge field—a consequence of the dual Higgs mechanism.

The equations of motion of the dual gauge field are

$$\partial_\mu \tilde{F}'^{\mu\nu} = q^2\phi_0^2\tilde{A}'^{\nu}, \tag{85}$$

and that for the static fields give

$$\nabla\cdot\vec{\tilde{B}} = \rho_m, \text{ and} -\nabla\times\vec{\tilde{E}} = \vec{j}_m, \tag{86}$$

where the magnetic monopole charge and current densities ρ_m, $\vec{j}_m$, respectively, are defined by the current density $j^\mu = q^2\phi_0^2\tilde{A}'^{\mu}$. So these equations govern a dual superconductor with the dual London equation $\nabla\times\vec{j}_m = (1/\lambda^2)\vec{\tilde{E}}$, where $\lambda = (q^2\phi_0^2)^{-1/2}$ is the penetration depth [86]. This scenario leads to the description of condensed magnetic monopoles and confined electric field, as we previously assumed.

4. Results and Analysis

Plotting the results of Equations (66), (67), (36), (68), (45), (46), (56), and (55) in Figures 1–8, we assume that $f_\alpha = \beta = 1$, $g/4\pi = \lambda = \pm 1$, and $N_c \gg 1$. Figure 1 shows graphically the relationship between the interquark potential $V_c(r, m_{q\bar{q}})$ with $(r, m_{q\bar{q}})$ for a heavy antiquark source. The graph shows a steady increase in the gradient from $m_{q\bar{q}1}$ to $m_{q\bar{q}3}$ representing an increase in the strength of confinement from $m_{q\bar{q}1}$ to $m_{q\bar{q}3}$. Figure 3 represents the graph of $\sigma_c(m_{q\bar{q}})$ against $m_{q\bar{q}}$; it shows a linear increase in $\sigma_c(m_{q\bar{q}})$ against $m_{q\bar{q}}$ with its foot intersecting the $\sigma_c(m_{q\bar{q}})$ axis at 1 indicating the strength of interaction even at $m_{q\bar{q}} = 0$. The linearity in $\sigma_c(m_{q\bar{q}})$ depicts the confinement that exist between the (anti-)quark pairs. Figure 2 shows the graph of the QCD-like vacuum which is equivalent to the tachyon potential. Tachyon condensation is related to monopole condensation which translates into confinement. The deeper the depth of the curve, the more condensed the tachyons and the stronger the strength of the confinement and the vice versa. Again, Figure 4 shows the relationship between the scalar potential $S(r, m_{q\bar{q}})$ with $(r, m_{q\bar{q}})$. We notice that the greater the quark mass, the deeper the depth of the curve and the smaller the minima of the curves representing faster gluon condensation. The above discussions so far are related to the IR regime. But, the same is true for Figures 5–8 which incorporate some UV characteristics; the only difference is that heavy quarks ($m_{q\bar{q}} \geq 4\text{GeV}$) are required to achieve confinement in this regime due to the UV characteristics. Considering all the factors discussed above, we can deduce that the vector potentials are dominant over the scalar potentials for light quarks in the IR regime and heavy quarks UV regime, respectively.

By way of analysis, we will compare the vector and the scalar confinements as captured in literature. The vector potential takes into account the angular momentum of the quarks while the scalar potentials do not. The scalar potential actually thrives on the basis that the angular momentum is partially eliminated. In the vector confinement, the energy of the quarks are carried by the gluons (string tension) whereas in the scalar confinement, the energy is centered on the quark coordinates. The scalar potential is most useful in a nonrotating quark frame while the vector potential is a viable option for a rotating quark frame. Obviously, the "Thomas precession" that gives rise to vector confinement differs significantly from the one that gives rise to the scalar confinement [3–5, 25–27].

The graph in Figure 1(a) is for the different values of $m_{q\bar{q}}$. It shows the strength of $q\bar{q}$ confinement for the different values of $m_{q\bar{q}}$ as their separation distance r varies. The graph shows a steady increase in its gradient as $m_{q\bar{q}}$ is increased from 0 to 0.7 GeV. By inference, the particles are strongly confined with increasing mass. Notwithstanding, a system of fermions remain confined even if the mass of the fermions is "removed" ($m_{q\bar{q}} = 0$) after confinement due to the *chromoelectric flux tube confinement*, in consistence with the QCD theory. The graph in Figure 1(b) is for the infinite limit of quark masses; it rises sharply, indicating confinement and flatten up shortly indicating hadronization. $\Lambda_\chi = 1\,\text{GeV}$ is the threshold mass; below which, quarks are classified as light and beyond which, they are classified as heavy.

The linear nature of the graph indicates that $q\bar{q}$ is confined for increasing $m_{q\bar{q}}$. The foot of the graph at 1 shows that the particles remain confined even at $m_{q\bar{q}} = 0$ in consistency with the QCD spectrum for heavy quarks.

The graph in Figure 2(a) is for the different values of $m_{q\bar{q}}$ to show how the tachyons condense with the increasing mass. Even though we find some tachyon condensate at $m_{q\bar{q}} = 0$, we can also see that the condensation is faster with the increasing mass. The deeper the depth of the graph, the more condensed the tachyons are and vice versa. The graph in Figure 2(b) represents the tachyon condensation for infinite $m_{q\bar{q}}$ limits. It shows stronger tachyon condensation.

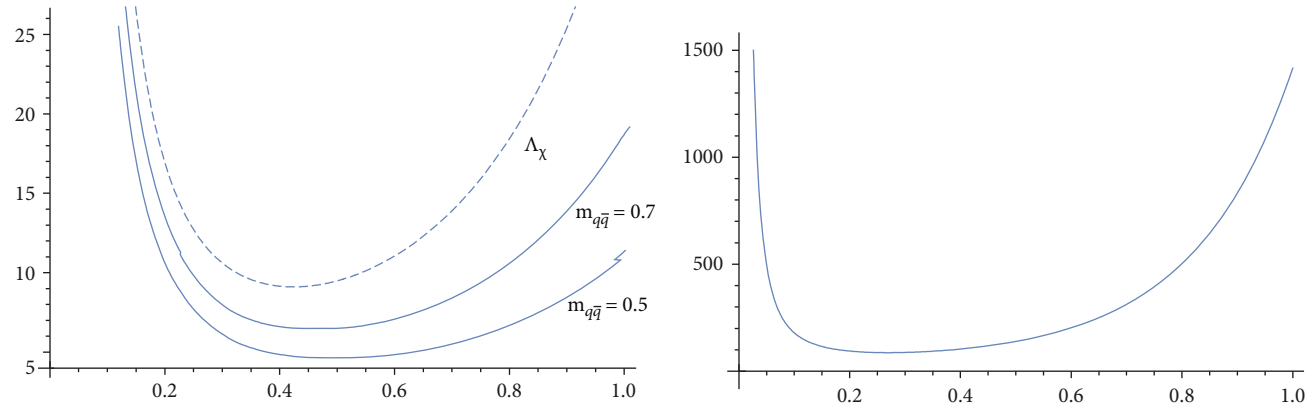

(a) Left panel (b) Right panel

FIGURE 4: A graph of the scalar potential $S(r, m_{q\bar{q}})$ against $(r, m_{q\bar{q}})$ for specific values of $m_{q\bar{q}}$ (a) and infinite $m_{q\bar{q}}$ (b).

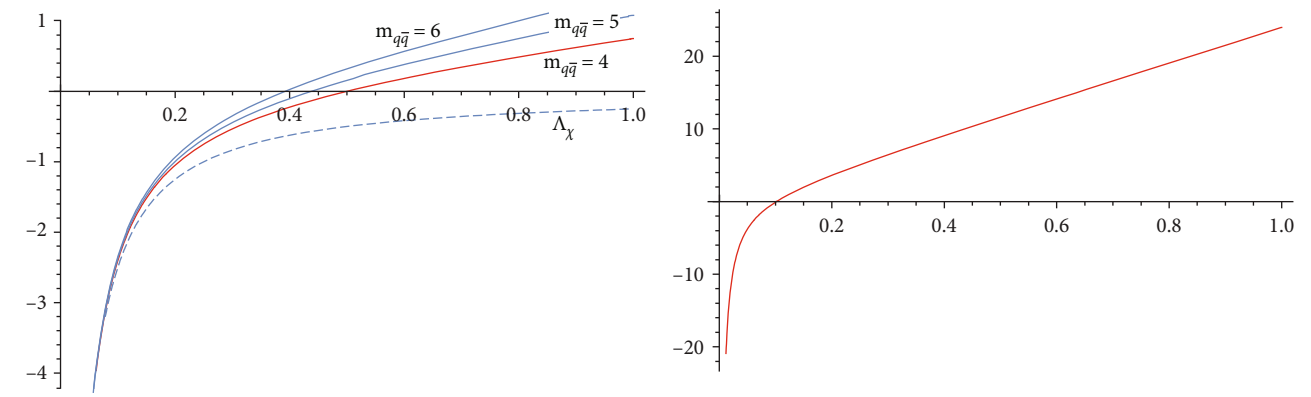

(a) Left panel (b) Right panel

FIGURE 5: A graph of the Cornell-like potential $V_s(r, m_{q\bar{q}})$ against $(r, m_{q\bar{q}})$ for specific values of $m_{q\bar{q}}$ (a) and infinite $m_{q\bar{q}}$ limit (b).

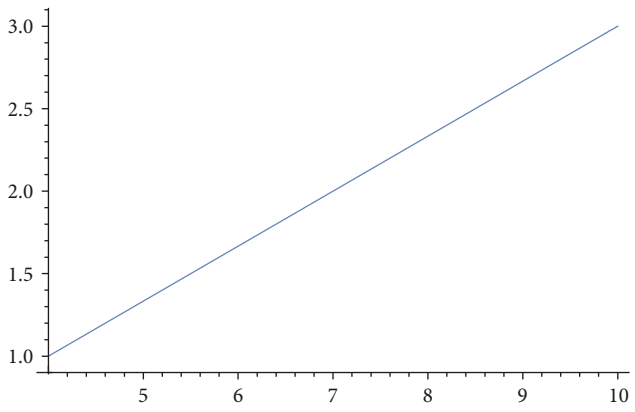

FIGURE 6: A graph of string tension $\sigma_s(m_{q\bar{q}})$ resulting from the Cornell-like potential against mass, $m_{q\bar{q}}$, for a heavy quark source.

The potential vanishes at $m_{q\bar{q}} = 0$, for both graphs, and increases in depth as $m_{q\bar{q}}$ increases as shown in Figure 4(a). The graph in Figure 4(b) has a deeper depth and represents stronger confinement. The $S(r, m_{q\bar{q}})$ deceases with mass from the left until it attains its minimum at $S(r, m_{q\bar{q}}) \longrightarrow 0$ and starts rising from the minimum towards the right; this is true for both graphs. The decrease implies stable confinement while the rise towards the right signifies degeneracy and screening of the static antiquark source. These are characteristics demonstrated by light mesons [66].

The graph in Figure 5(a) rises steadily with the increasing mass indicating strong confinement with the increasing mass while the graph in Figure 4(b) shows stronger confinement with an infinite increase in the quark mass.

The graph shows strong confinement with increasing quark mass $m_{q\bar{q}}$.

The potential vanishes at $m_{q\bar{q}} = 0$. The scalar potential increases with the increasing mass. Thus, the higher the quark mass, the more likely the quarks will be confined even at higher energy regimes (small r) for finite quark masses as shown in Figure 7(a). For infinite quark masses (right), the scalar potential also increases as $m_{q\bar{q}} \longrightarrow \infty$, consequently confining the quarks at high energy regimes.

The graph in the left panel shows a slight increase in tachyon condensation with the increasing quark mass, so the increase in the quark mass goes into confining the quarks at higher energies $r \longrightarrow 0$. Likewise, in the right panel, the tachyon condensation increases steadily as $m_{q\bar{q}} \longrightarrow \infty$ resulting into confinement at higher energy regimes.

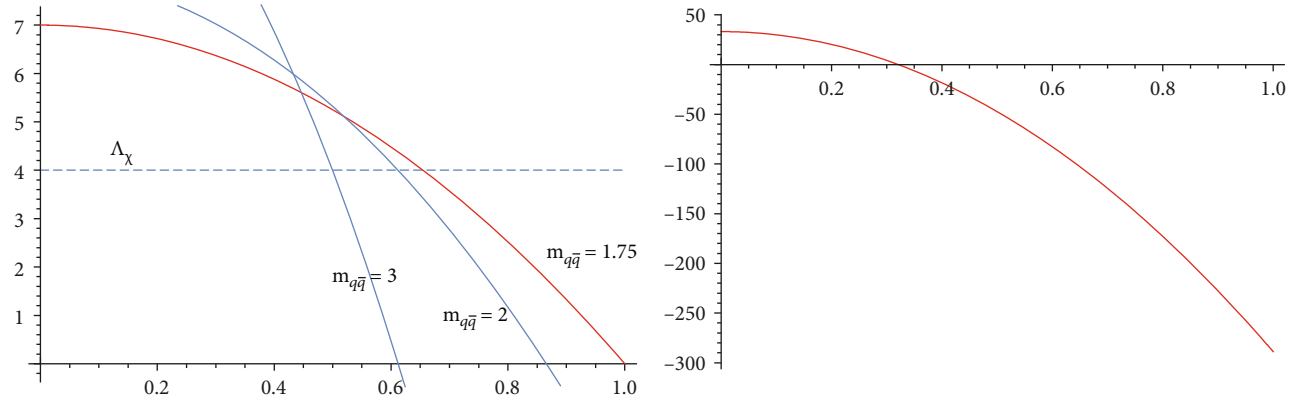

(a) Left panel (b) Right panel

FIGURE 7: A graph of the scalar potential $S_s(r, m_{q\bar{q}})$ against $(r, m_{q\bar{q}})$ for specific values of $m_{q\bar{q}}$ (a) and infinite $m_{q\bar{q}}$ limit (b).

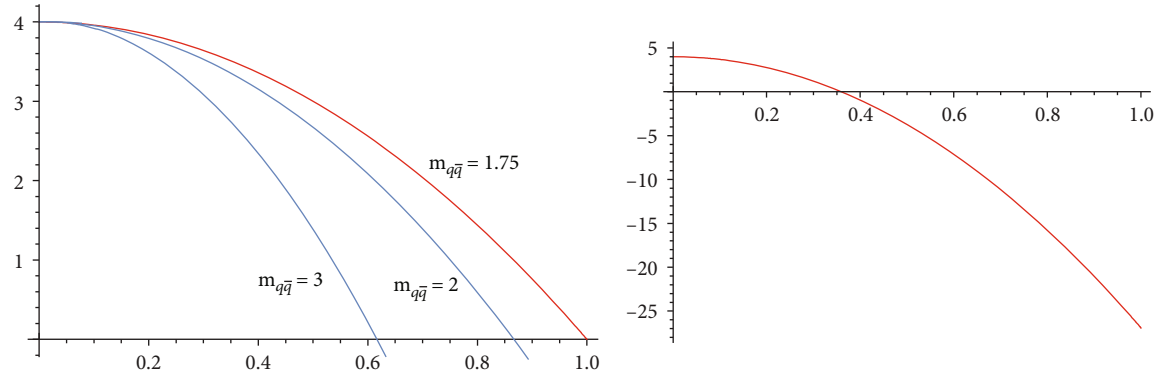

(a) Left panel (b) Right panel

FIGURE 8: A graph of color dielectric function $G_s(r, m_{q\bar{q}})$ against $(r, m_{q\bar{q}})$ for specific values of $m_{q\bar{q}}$ (a) and infinite $m_{q\bar{q}}$ (b).

5. Conclusions

The model gives an insightful details about the QCD theory in both the IR and the UV regimes making it more efficient for consideration. We have calculated the net potential of the slowly moving quarks inside the hadron, vector potential, scalar potential energy, net potential energy, and the string tensions associated with them in both regimes. Vector and scalar glueball masses which are consequences of the IR regime were also studied and their values for $f_\alpha = 0.5$ (consequently, $\phi_0 = 500$ MeV) and σ_c~1 GeV/fm was calculated and compared with the existing QCD lattice results for quenched (no quark fluctuation) and unquenched (hybrid fluctuation) approximations, respectively.

The dominance of the vector potential expected in the QCD theory was clearly demonstrated by computing the coupling strengths ξ for both the vector and the scalar potentials. We also find that the scalar potential (energy) must be strongly coupled in order to coexist with the vector potential (energy) which needs no coupling at all in this model framework. The vector and the scalar potentials should be understood as resulting from relativistic spin-orbit corrections at short and long ranges, respectively. The vector potential (energy) shows confinement of *chromoelectric flux* at zero mass, but the scalar potential (energy) vanishes at the same mass. Thus, the vector potential (energy) is more suitable for confining light quarks while at least a heavy source is required to obtain scalar potential (energy). Furthermore, we established the relation between tachyon condensation, dual Higgs mechanism, QCD monopole condensation [87], and confinement. Finally, we intend to continue our series on this subject by studying confinement of fermions at a finite temperature.

Data Availability

The data will be available upon request.

Conflicts of Interest

The authors declare that they have no conflicts of interest.

Acknowledgments

We would like to thank CNPq, CAPES, and CNPq/PRONEX/FAPESQ-PB (Grant no. 165/2018) for the partial financial support. FAB acknowledges support from CNPq (Grant no. 312104/2018-9).

References

[1] S. Eidelman, B. K. Heltsley, J. J. Hernandez-Rey, S. Navas, and C. Patrignani, "Developments in heavy quarkonium spectroscopy," 2012, http://arxiv.org/abs/1205.4189.

[2] N. Brambilla, M. Krämer, R. Mussa et al., *Heavy Quarkonium physics*, CERN, Geneva, 2005, http://arxiv.org/abs/hep-ph/0412158.

[3] A. S. de Castro, "Confinement of fermions by mixed vector–scalar linear potentials in two- dimensional space–time," *Physics Letters A*, vol. 305, no. 3-4, pp. 100–104, 2002.

[4] A. S. de Castro, "Erratum to: "Confinement of fermions by mixed vector–scalar linear potentials in two-dimensional space–time": [Phys. Lett. A 305 (2002) 100]," *Physics Letters A*, vol. 308, no. 1, p. 80, 2003.

[5] S. Coleman, R. Jackiw, and L. Susskind, "Charge shielding and quark confinement in the massive schwinger model," *Annals of Physics*, vol. 93, no. 1-2, pp. 267–275, 1975.

[6] B. J. Harrington, S. Y. Park, and A. Yildiz, "Spectrum of Heavy Mesons ine+e−Annihilation," *Physical review letters*, vol. 34, no. 3, pp. 168–171, 1975.

[7] E. Eichten, K. Gottefried, T. Kinoshita, J. Kogut, K. D. Lane, and T.-M. Yan, "Spectrum of Charmed Quark-Antiquark Bound States," *Physical review letters*, vol. 34, no. 6, pp. 369–372, 1975.

[8] H. J. W. Müller-Kirsten, "Quark confinement, rising trajectories, and asymptotic behavior of form factors," *Physical Review D*, vol. 12, no. 4, pp. 1103–1122, 1975.

[9] J. F. Gunion and R. S. Willey, "Hadronic spectroscopy for a linear quark containment potential," *Physical Review D*, vol. 12, no. 1, pp. 174–186, 1975.

[10] K. S. Jhung, K. H. Chung, and R. S. Willey, "Relativistic quasipotential calculation of quark-model meson masses," *Physical Review D*, vol. 12, no. 7, pp. 1999–2001, 1975.

[11] P. Bicudo and G. M. Marques, "Chiral Symmetry Breaking and Scalar Confinement," 2003, http://arxiv.org/abs/hep-ph/0309231.

[12] R. Dick, "Vector and scalar confinement in gauge theory with a dilaton," *Physics letters B*, vol. 409, no. 1-4, pp. 321–324, 1997.

[13] W. Lucha, F. F. Schöberl, and D. Gromes, "Bound states of quarks," *Physics reports*, vol. 200, no. 4, pp. 127–240, 1991.

[14] L. B. Castro, A. S. de Castro, and M. B. Hott, "Bounded solutions of fermions in the background of mixed vector-scalar Pöschl-Teller–like potentials," *Europhysics Letters (EPL)*, vol. 77, no. 2, p. 20009, 2007.

[15] M. Creutz, "Monte Carlo study of quantized SU(2) gauge theory," *Physical Review D*, vol. 21, no. 8, pp. 2308–2315, 1980.

[16] M. Lüscher, K. Symanzik, and P. Weisz, "Anomalies of the free loop wave equation in the WKB approximation," *Nuclear Physics B*, vol. 173, no. 3, pp. 365–396, 1980.

[17] E. Majorana, "Teoria simmetrica dell'elettrone e del positrone," *Il Nuovo Cimento*, vol. 14, no. 4, pp. 171–184, 1937.

[18] P. A. M. Dirac, "The quantum theory of the electron," *Proceedings of the Royal Society of London Series A, Containing Papers of a Mathematical and Physical Character*, vol. 117, no. 778, pp. 610–624, 1997.

[19] R. Dick, "The Coulomb potential in gauge theory with a dilaton," *Physics letters B*, vol. 397, no. 3-4, pp. 193–196, 1997.

[20] M. Cvetic and A. A. Tseytlin, "Charged string solutions with dilaton and modulus fields," *Nuclear Physics B*, vol. 416, no. 1, pp. 137–172, 1994.

[21] A. Sen, "Tachyon Condensation on the Brane Antibrane System," *Journal of High Energy Physics*, vol. 1998, 1998.

[22] H. J. Rothe, "Lattice Gauge Theories," in *World Scientific Lecture Notes in Physics 43*, 1992.

[23] O. Bergman, K. Hori, and P. Yi, "Confinement on the brane," *Nuclear Physics B*, vol. 580, no. 1-2, pp. 289–310, 2000.

[24] V. Mathieu, N. Kochelev, and V. Vento, "The Physics of Glueballs," *International Journal of Modern Physics E*, vol. 18, no. 1, pp. 1–49, 2009.

[25] G. S. Bali and P. Boyle, "Lattice potential investigation of quark mass and volume dependence of theϒspectrum," *Physical Review D*, vol. 59, no. 11, p. 114504, 1999.

[26] N. Brambilla and B. M. Prosperi, "Testing relativistic corrections to the qq potential on the heavy quarkonium spectrum," *Physics letters B*, vol. 236, no. 1, pp. 69–75, 1990.

[27] C. Olson, M. G. Olsson, and K. Williams, "QCD, relativistic flux tubes, and potential models," *Physical Review D*, vol. 46, p. 4307, 1992.

[28] A. B. Henriques, B. H. Kellet, and R. G. Moorhouse, "Radiative transitions and the P wave levels in charmonium," *Physics letters B*, vol. 64, no. 1, pp. 85–92, 1976.

[29] T. J. Allen, M. G. Olsson, and S. Veseli, "From scalar to string confinement," *Physical Review D*, vol. 62, no. 9, article 094021, 2000.

[30] E. Eichten and F. Feinberg, "Spin-dependent forces in quantum chromodynamics," *Physical Review D*, vol. 23, no. 11, pp. 2724–2744, 1981.

[31] D. Gromes, "Relativistic corrections to the long-range quark antiquark potential electric flux tubes, and area law," *Zeitschrift für Physik C Particles and Fields*, vol. 22, no. 3, pp. 265–270, 1984.

[32] A. Barchielli, E. Montaldi, and G. M. Prosperi, "On a systematic derivation of the quark-antiquark potential," *Nuclear Physics B*, vol. 296, no. 3, pp. 625–656, 1988.

[33] A. Barchielli, N. Brambilla, and G. M. Prosperi, "Relativistic corrections to the quark-antiquark potential and the quarkonium spectrum," *Il Nuovo Cimento A*, vol. 103, no. 1, pp. 59–83, 1989.

[34] L. Wilets, *Non topological solutions*, World Scientific, Singapore, 1998.

[35] S. Maedan, Y. Matsubara, and T. Suzuki, "Abelian Confinement Mechanism and the QCD Vacuum," *Progress in theoretical physics*, vol. 84, no. 1, pp. 130–141, 1990.

[36] T. D. Lee, *Particle physics and introduction to field theory*, Harwood Academic, New York, 1981.

[37] G. S. Bali, V. Bornyakov, M. Müller-Preussker, and K. Schilling, "Dual superconductor scenario of confinement: A systematic study of Gribov copy effects," *Physical Review D*, vol. 54, no. 4, pp. 2863–2875, 1996.

[38] H. Shiba and T. Suzuki, "Monopoles and string tension in SU(2) QCD," *Physics letters B*, vol. 333, no. 3-4, pp. 461–466, 1994.

[39] N. Sakumichi and H. Suganuma, "Perfect Abelian dominance of quark confinement in SU(3) QCD," *Physical Review D*, vol. 90, no. 11, p. 111501, 2014.

[40] N. Sakumichi and H. Suganuma, "Three-quark potential and Abelian dominance of confinement in SU(3) QCD," *Physical Review D*, vol. 92, no. 3, article 034511, 2015.

[41] T. Suzuki, "Abelian Confinement Mechanism in QCD," *Progress in theoretical physics*, vol. 81, no. 4, pp. 752–757, 1989.

[42] A. Chodos, R. L. Jaffe, K. Jonhson, C. B. Thorn, and V. F. Weisskopf, "New extended model of hadrons," *Physical Review D*, vol. 9, no. 12, pp. 3471–3495, 1974.

[43] W. A. Bardeen, M. S. Chanowitz, S. D. Drell, M. Weinstein, and T. M. Yan, "Heavy quarks and strong binding: A field theory of hadron structure," *Physical Review D*, vol. 11, no. 5, pp. 1094–1136, 1975.

[44] R. Friedberg and T. D. Lee, "Fermion Field Nontopological Solitons," *Physical Review D*, vol. 15, p. 1964, 1997.

[45] D. Atkinson and P. W. Johnson, "Current and constituent quark masses: Beyond chiral-symmetry breaking," *Physical Review D*, vol. 41, no. 5, pp. 1661–1666, 1990.

[46] M. Tanabashi, K. Hagiwara, K. Hikasa et al., "Review of Particle Physics," *Physical Review D*, vol. 98, no. 3, article 030001, 2018.

[47] K. Melnikov and T. van Ritbergen, "The three-loop relation between the MS and the pole quark masses," *Physics Letters B*, vol. 482, no. 1-3, pp. 99–108, 2000.

[48] T. Hatsuda and T. Kunihiro, "QCD phenomenology based on a chiral effective Lagrangian," *Physics Reports*, vol. 247, no. 5-6, pp. 221–367, 1994.

[49] A. V. Manohar and H. Georgi, "Chiral quarks and the nonrelativistic quark model," *Nuclear Physics B*, vol. 234, no. 1, pp. 189–212, 1984.

[50] F. A. Brito, M. L. F. Freire, and W. Serafim, "Confinement and screening in tachyonic matter," *European physical journal C: Particles and fields*, vol. 74, no. 12, p. 3202, 2014.

[51] D. Bazeia, F. A. Brito, W. Freire, and R. F. Ribeiro, "Confinement from new global defect structures," *The European physical journal C*, vol. 40, no. 4, pp. 531–537, 2005.

[52] A. Issifu and F. A. Brito, "The (De)confinement Transition in Tachyonic Matter at Finite Temperature," *Advances in High Energy Physics*, vol. 2019, Article ID 9450367, 9 pages, 2019.

[53] J. Ellis, "Aspects of conformal symmetry and chirality," *Nuclear Physics B*, vol. 22, no. 2, pp. 478–492, 1970.

[54] R. J. Crewther, "Broken scale invariance and the width of a single dilaton," *Physics Letters B*, vol. 33, no. 4, pp. 305–308, 1970.

[55] R. J. Crewther, "Nonperturbative Evaluation of the Anomalies in Low-Energy Theorems," *Physical Review Letters*, vol. 28, no. 21, pp. 1421–1424, 1972.

[56] M. S. Chanowitz and J. Ellis, "Canonical anomalies and broken scale invariance," *Physics Letters B*, vol. 40, no. 3, pp. 397–400, 1972.

[57] M. S. Chanowitz and J. Ellis, "Canonical Trace Anomalies," *Physical Review D*, vol. 7, no. 8, pp. 2490–2506, 1973.

[58] D. Kharzeev, E. Levin, and K. Tuchin, "Classical gluodynamics in curved space–time and the soft pomeron," *Physics letters B*, vol. 547, no. 1-2, pp. 21–30, 2002.

[59] M. Rosina, A. Schuh, and H. J. Pirner, "Lattice QCD and the soliton bag model," *Nuclear Physics A*, vol. 448, no. 4, pp. 557–566, 1986.

[60] S. Geltman, "Bound States in Delta Function Potentials," *Journal of Atomic, Molecular, and Optical Physics*, vol. 2011, article 573179, 4 pages, 2011.

[61] M. Gabella, *Tachyon condensation in open string field theory*, University of Oxford, 2008.

[62] A. Sen, "Tachyon Matter," *Journal of High Energy Physics*, vol. 2002, no. 7, p. 065, 2002.

[63] A. D. Alhaidari, H. Bahlouli, and A. Al-Hasan, "Dirac and Klein–Gordon equations with equal scalar and vector potentials," *Physics Letters A*, vol. 349, no. 1-4, pp. 87–97, 2006.

[64] A. Sen, "Rolling Tachyon," *Journal of High Energy Physics*, vol. 2002, no. 4, p. 048, 2002.

[65] T. J. Allen, M. G. Olsson, S. Veseli, and K. Williams, "Quark confinement dynamics," *Physical Review D*, vol. 55, no. 9, pp. 5408–5413, 1997.

[66] E. Eichten, K. Gottfried, T. Kinoshita, K. D. Lane, and T. . M. Yan, "Charmonium: The model," *Physical review D*, vol. 17, no. 11, pp. 3090–3117, 1978.

[67] S. Narison, "Light and heavy quark masses, test of PCAC and flavour breakings of condensates in QCD," *Physics letters B*, vol. 216, no. 1-2, pp. 191–197, 1989.

[68] G. S. Bali, "QCD forces and heavy quark bound states," *Physics Reports*, vol. 343, no. 1-2, pp. 1–136, 2001.

[69] S. Aoki, G. Boyd, R. Burkhalter et al., "The static quark potential in full QCD," *Nuclear Physics B - Proceedings Supplements*, vol. 73, no. 1-3, pp. 216–218, 1999.

[70] H.-W. Ke, Z. Li, J.-L. Chen, Y.-B. Ding, and X.-Q. Li, "Symmetry of Dirac Equation and Corresponding Phenomenology," *International Journal of Modern Physics A*, vol. 25, no. 6, pp. 1123–1134, 2010.

[71] W. Greiner, *Relativistic quantum mechanics*, Springer, Berlin, 2000.

[72] M. R. Pennington, "Glueballs : the Naked Truth," 1998, http://arxiv.org/abs/hep-ph/9811276.

[73] J. Sexton, A. Vaccarino, and D. Weingarten, "Numerical Evidence for the Observation of a Scalar Glueball," *Physical review letters*, vol. 75, no. 25, pp. 4563–4566, 1995.

[74] Y. Chen, A. Alexandru, S. J. Dong et al., "Glueball spectrum and matrix elements on anisotropic lattices," *Physical Review D*, vol. 73, no. 1, article 014516, 2006.

[75] H. Pagels, "Dynamical chiral symmetry breaking in quantum chromodynamics," *Physical Review D*, vol. 19, no. 10, pp. 3080–3090, 1979.

[76] F. Giacosa, J. Sammet, and S. Janowski, "Decays of the vector glueball," *Physical Review D*, vol. 95, no. 11, p. 114004, 2017.

[77] M. Ablikim, M. N. Achasov, S. Ahmed et al., "Evidence of Two Resonant Structures ine+e−→π+π−hc," *Physical review letters*, vol. 118, no. 9, p. 9, 2017.

[78] O. Andreev and V. I. Zakharov, "The spatial string tension, thermal phase transition, and AdS/QCD," *Physics letters B*, vol. 645, no. 5-6, pp. 437–441, 2007.

[79] R. Jackiw, "Functional evaluation of the effective potential," *Physical Review D*, vol. 9, no. 6, pp. 1686–1701, 1974.

[80] M. J. Strassler, *On confinement duality*, University of Pennsylvania, Philadelphia, USA, 2001.

[81] M. Thorsrud, "Quintessence with Kaluza-Klein type couplings to matter and an isotropy-violating vector field," http://arxiv.org/abs/1303.2469.

[82] H. Suganuma, S. Sasaki, and H. Toki, "Color confinement, quark pair creation and dynamical chiral-symmetry breaking in the dual Ginzburg-Landau theory," *Nuclear Physics B*, vol. 435, no. 1-2, pp. 207–240, 1995.

[83] H. Suganuma, S. Sasaki, and H. Toki, "Quark confinement and Hadron Spectrum," in *Proceedings of the International Conference (World Scientific, 1993)*, Como, Italy, 1993.

[84] H. Toki, H. Suganuma, and S. Sasaki, "Magnetic monopole condensation for confinement and chiral symmetry breaking," *Nuclear Physics A*, vol. 577, no. 1-2, pp. 353–360, 1994.

[85] H. Suganuma, S. Sasaki, H. Toki, and H. Ichie, "Dual Higgs Mechanism for Quarks in Hadrons," *Progress of Theoretical Physics Supplement*, vol. 120, pp. 57–73, 1995.

[86] C. Quigg, *Gauge theories of strong, weak, and electromagnetic interactions*, Princeton University Press, New Jersey, 2013.

[87] D. Griffiths, *Introduction to elementary particles*, WILEY-VCH Verlag GmbH and Co. KGaA, Weinheim, 2008.